DEUTSCHES ELEKTRONEN-SYNCHROTRON
Ein Forschungszentrum der Helmholtz-Gemeinschaft

DESY 19-093
BONN-TH 2019-04
KA-TP-09-2019
IFT-UAM/CSIC-19-075
arXiv:2005.14536
June 2019

HL-LHC and ILC Sensitivities in the Hunt for Heavy Higgs Bosons

H. Bahl, T. Stefaniak, G. Weiglein

Deutsches Elektronen-Synchrotron DESY, Hamburg

P. Bechtle

Physikalisches Insitut, Universität Bonn

S. Heinemeyer

Instituto de Física Teórica, (UAM/CSIC), Universidad Autónoma de Madrid, Cantoblanco, Madrid, Spain

and

Campus of International Excellence UAM+CSIC, Cantoblanco, Madrid, Spain

and

Instituto de Física de Cantabria (CSIC-UC), Santander, Spain

S. Liebler

Institut für Theoretische Physik, Karlsruher Institut für Technologie (KIT), Karlsruhe

ISSN 0418-9833

NOTKESTRASSE 85 - 22607 HAMBURG

DESY, Notkestraße 85, D-22607 Hamburg, Germany

Physikalisches Institut der Universität Bonn, Nußallee 12, D-53115 Bonn, Germany

Instituto de Física Teórica, (UAM/CSIC), Universidad Autónoma de Madrid, Cantoblanco, E-28049 Madrid, Spain

Campus of International Excellence UAM+CSIC, Cantoblanco, E-28049, Madrid, Spain

Instituto de Física de Cantabria (CSIC-UC), E-39005 Santander, Spain

Institute for Theoretical Physics (ITP), Karlsruhe Institute of Technology, D-76131 Karlsruhe, Germany

Abstract

M_h^{125} M_h^{125} χ

β $M_{h,\mathrm{EFT}}^{125}$ $M_{h,\mathrm{EFT}}^{125}$ χ

$\boldsymbol{H/A \to bb}$

τ

h

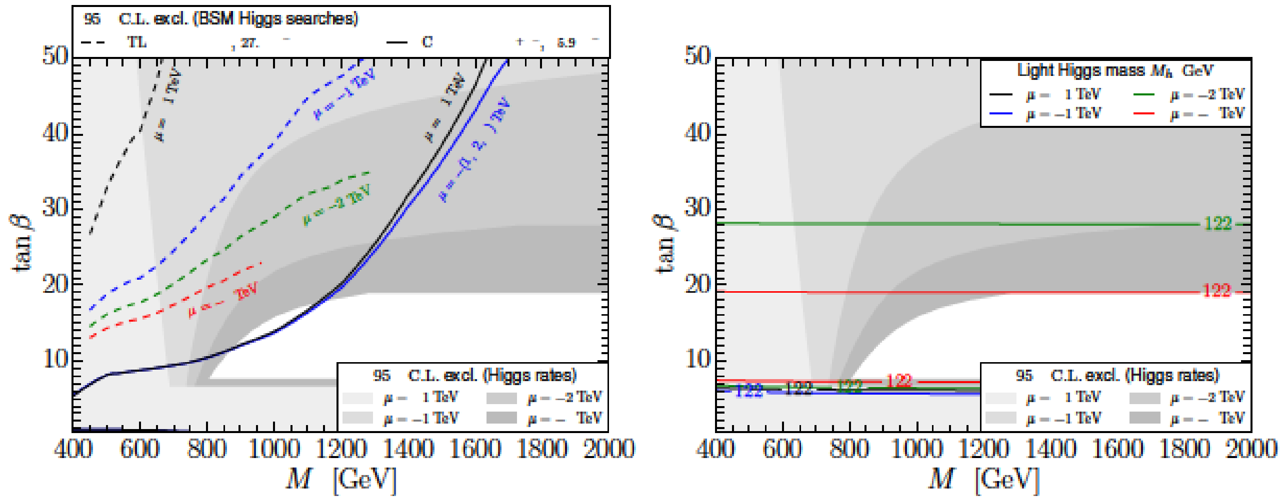

Figure 1: M_h^{125} scenario in comparison with the proposed new $M_h^{125}(\mu = -2\,\text{TeV})$ scenario and the other choices of $\mu = -1\,\text{TeV}, -3\,\text{TeV}$, shown in the $(M_A, \tan\beta)$ parameter plane. *Left panel*: current experimental constraints from heavy Higgs searches in the $b\bar{b}$ [64] (dashed lines) and $\tau^+\tau^-$ [65] (solid lines) final state and 125 GeV Higgs rate measurements (gray filled regions); *Right panel*: Contours for the lowest acceptable value of the light-Higgs boson mass, $M_h = 122\,\text{GeV}$ (taking into account a theory uncertainty of $\pm 3\,\text{GeV}$), with the Higgs rate constraints (from the left panel) superimposed.

CMS $pp \to H/A \to \tau^+\tau^-$ search [65] with 35.9 fb^{-1} of data, both at a center-of-mass energy of 13 TeV, using `HiggsBounds` [66–71]. The indirect constraints from Higgs rate measurements are evaluated with `HiggsSignals` (version `2.3.0`) [72,73] by means of a negative log-likelihood ratio (LLR) test with the SM as alternative hypothesis, and approximating the likelihood with a χ^2 function. This test uses Run-1 [3] and recent Run-2 results up to around 80 fb^{-1} from ATLAS [74] and CMS [75–84]. Fig. 1 (*left*) clearly illustrates that $pp \to H/A \to b\bar{b}$ searches become more sensitive for scenarios with large negative μ values due to the enhancement of the bottom-quark Yukawa coupling, as the excluded regions probe lower values of $\tan\beta$ for larger negative μ values.[4] It is noteworthy that the exclusion limit from $pp \to H/A \to \tau^+\tau^-$ searches does not vary significantly with μ.[5] This is because the $pp \to H/A \to b\bar{b}$ signal rate profits from an enhancement in the production (in the $gg \to b\bar{b}H/A$ production mode) *and* in the decay branching ratio (BR) of the $H/A \to b\bar{b}$ decay, while the $pp \to H/A \to \tau^+\tau^-$ signal rate only gains from the enhancement in the production rate whereas in combination with the decay rate $\text{BR}(H/A \to \tau^+\tau^-)$ a large compensation of Δ_b effects occurs [85]. Still, we observe that heavy Higgs-boson searches in the $b\bar{b}$ final state cover significantly less parameter space in

[4]The exclusion lines for $\mu = -2\,\text{TeV}$ and $-3\,\text{TeV}$ terminate, as for larger $\tan\beta$ values the light Higgs boson mass quickly decreases (see also the right panel of Fig. 1) and the prediction of Higgs-boson masses is affected by large uncertainties.

[5]The exclusion contours derived from the CMS $pp \to H/A \to \tau^+\tau^-$ search are practically identical for the choices $\mu = -1$, -2 and $-3\,\text{TeV}$, and therefore plotted as a single contour.

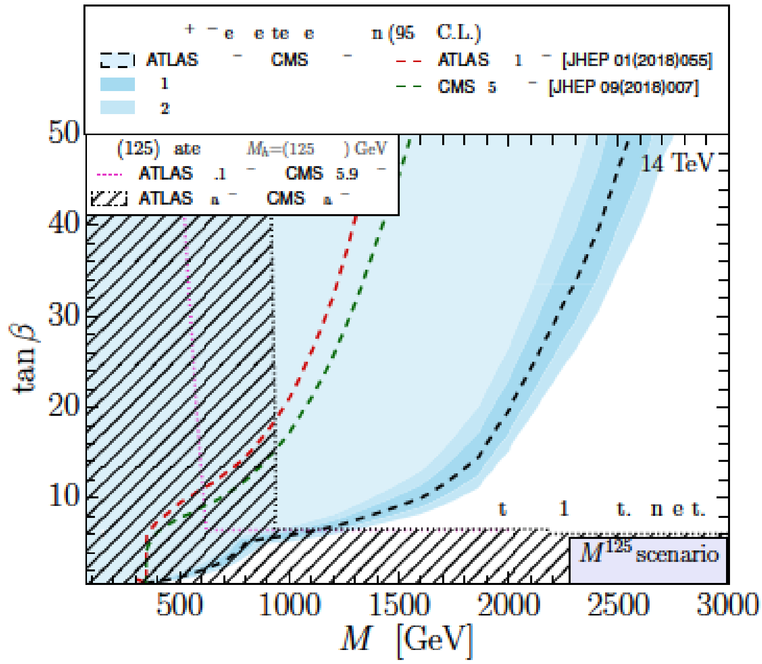

Figure 2: HL-LHC projections in the M_h^{125} scenario, assuming YR18 systematic uncertainties (scenario S2 in Ref. [15]). The dashed black curve and blue filled region indicate the expected HL-LHC reach via direct heavy Higgs searches in the $\tau^+\tau^-$ channel with 6 ab^{-1} of data (with the dark blue regions indicating the 1 and 2σ uncertainty), whereas the red and green dashed lines show the expected limit from current searches in this channel by ATLAS [106] and CMS [65], respectively. The current and future HL-LHC sensitivity via combined ATLAS and CMS Higgs rate measurements is shown as magenta and black dotted contours, respectively (the latter being accompanied with a hatching of the prospectively excluded region).

sufficient to probe parameter regions that are not covered by the direct Higgs searches (black dashed line). Those direct searches in the $\tau^+\tau^-$ final state will probe the parameter space up to $M_A \lesssim 2.5\,\text{TeV}$ for the highest displayed $\tan\beta$ values of $\tan\beta \sim 50$. At $\tan\beta = 20$ the reach extends up to $M_A \lesssim 2000\,\text{GeV}$. The change in the curvature of the black dashed line around $M_A \sim 1.9\,\text{TeV}$ can be understood from the fact that for larger values of M_A decays of H and A into electroweakinos open, thus diminishing the event yield of the $\tau^+\tau^-$ final state. The kink in the exclusion boundary at $M_A \sim 800$ GeV is caused by a transition of the main production channel from gluon fusion (low $\tan\beta$ values) to bottom quark associated production (high $\tan\beta$ values).[10] In this scenario the prospective combined sensitivity from direct and indirect searches in the absence of a signal would yield a lower bound on M_A of about $M_A \gtrsim 1200\,\text{GeV}$. In order to correctly interpret this result, the following should be taken into account. As explained above, this bound is *not* a consequence of prospective Higgs signal strength measurements at

[10] It should be kept in mind that for the projected $H/A \to \tau^+\tau^-$ search sensitivity we used the one-dimensional profiled cross section limits for the two relevant production modes.

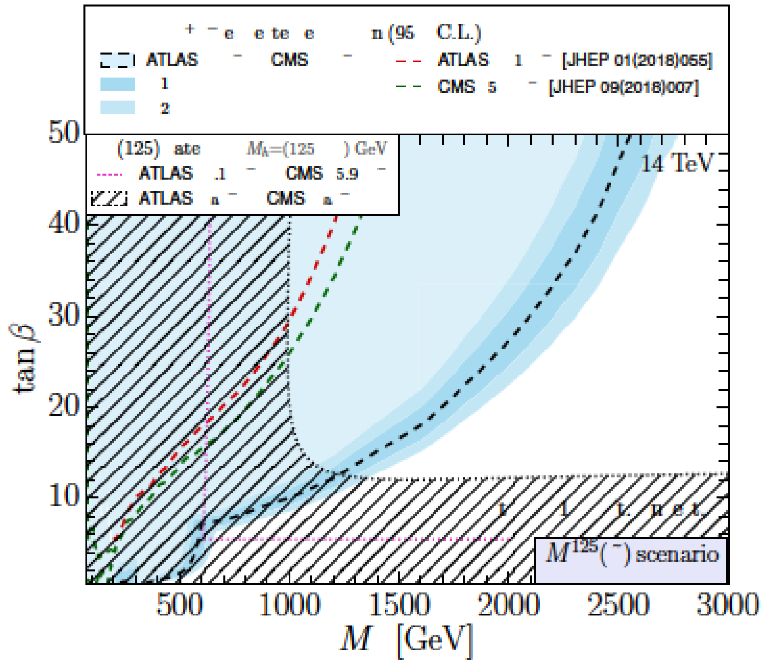

Figure 3: HL-LHC projections in the $M_h^{125}(\tilde{\chi})$ scenario with the same color coding as in Fig. 2.

the HL-LHC, but it is rather driven by the direct Higgs search reach in combination with the Higgs-mass prediction. Since by definition for this benchmark scenario all parameters except M_A and $\tan\beta$ are set to fixed values, the adopted theoretical uncertainty of the Higgs-mass prediction has a major impact on the resulting bound. For a smaller theoretical uncertainty the allowed region in this scenario would be shifted to larger $\tan\beta$ values, so that the lower bound on M_A would rise to values above 2 TeV. On the other hand, in scenarios where the prediction for the mass of the light Higgs boson is compatible with the measured Higgs-boson mass also for low $\tan\beta$ values, the indirect constraints on M_A from the rate measurements can exceed the sensitivity from the direct searches (see the discussion below).

The picture is somewhat different in the $M_h^{125}(\tilde{\chi})$ scenario. Here the large branching ratio of the heavy neutral Higgs boson decaying to charginos and neutralinos already at lower values of M_A leads to a strongly reduced direct reach of $H/A \to \tau^+\tau^-$ searches. The kink in the exclusion boundary at $M_A \sim 600$ GeV is as in Fig. 2 caused by a transition of the most sensitive production channel from gluon fusion (at low $\tan\beta$ values) to bottom quark associated production (at high $\tan\beta$ values). At $\tan\beta = 20$ the reach in the $M_h^{125}(\tilde{\chi})$ scenario is significantly reduced to $M_A \lesssim 1700$ GeV compared to the M_h^{125} scenario with $M_A \lesssim 2000$ GeV. On the other hand, at large values of $\tan\beta \sim 50$ and thus large M_A the reach is only slightly weaker than in the M_h^{125} scenario, as for those M_A values in both scenarios decays into electroweakinos are kinematically open. In order to further strengthen the impact of direct searches it would be useful to supplement the searches in the $\tau^+\tau^-$ and $b\bar{b}$ final states with dedicated searches for the decays of H and A to charginos, neutralinos and in general also to sleptons. Higgs rate

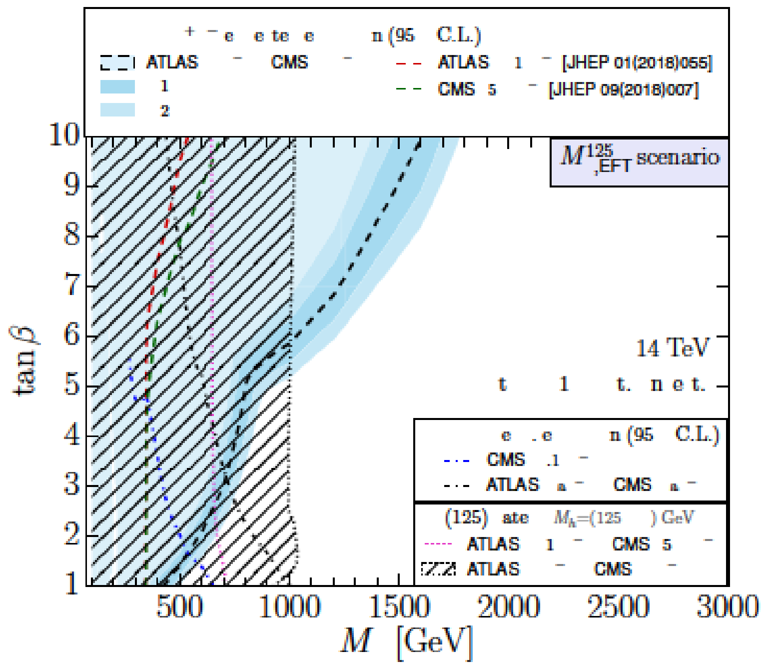

Figure 4: HL-LHC projections in the $M_{h,\mathrm{EFT}}^{125}$ scenario with the same color coding as in Fig. 2. The blue and black dash-dotted lines show the current CMS [88] and future HL-LHC expected 95% C.L. limit from a combination of $H \to hh$ searches (see Sec. 3 for details).

largest coverage for $\tan\beta$ values up to $\tan\beta \sim 5.5$, while for higher values of $\tan\beta$ the direct searches for heavy Higgs bosons in the $\tau^+\tau^-$ final state have the best prospects.

In order to cover the low-$\tan\beta$ region, further experimental sensitivity studies for direct searches for $H/A \to t\bar{t}$, $H \to hh$ and $A \to Zh$ decays as well as heavy Higgs boson decays into electroweakinos are of interest (see Refs. [87, 95] for recent theorists' projections of $H/A \to t\bar{t}$ and $H \to hh$, and Ref. [15] for experimental projections in different scenarios). The searches for decays to electroweakinos are of particular importance in both the $M_h^{125}(\tilde{\chi})$ and the $M_{h,\mathrm{EFT}}^{125}(\tilde{\chi})$ scenario, see also Ref. [10, 11, 108].

We now turn to the second EFT scenario, $M_{h,\mathrm{EFT}}^{125}(\tilde{\chi})$, with a light EWino spectrum. As for the case of the $M_h^{125}(\tilde{\chi})$ scenario discussed above, the HL-LHC measurement of the di-photon Higgs-boson signal rate has the potential to set a lower bound on $\tan\beta$ for the chosen values of the chargino masses. In fact, restricting ourselves to the $\tan\beta$ range between 1 and 10 that was originally proposed for this scenario, the entire $(M_A, \tan\beta)$ plane of the $M_{h,\mathrm{EFT}}^{125}(\tilde{\chi})$ scenario can be probed by the HL-LHC measurement of the di-photon Higgs-boson signal rate. Accordingly, this parameter plane could be excluded at the HL-LHC if no deviation from the SM prediction is observed. Therefore, instead of displaying the $(M_A, \tan\beta)$ plane, we instead investigate the reach of the HL-LHC in the (M_2, μ) parameter plane, where M_2 is the soft-breaking wino mass parameter and μ the Higgs mixing parameter. This is shown in Fig. 5, where we highlight the prospective 2σ excluded region, assuming HL-LHC Higgs signal rate measurements that agree

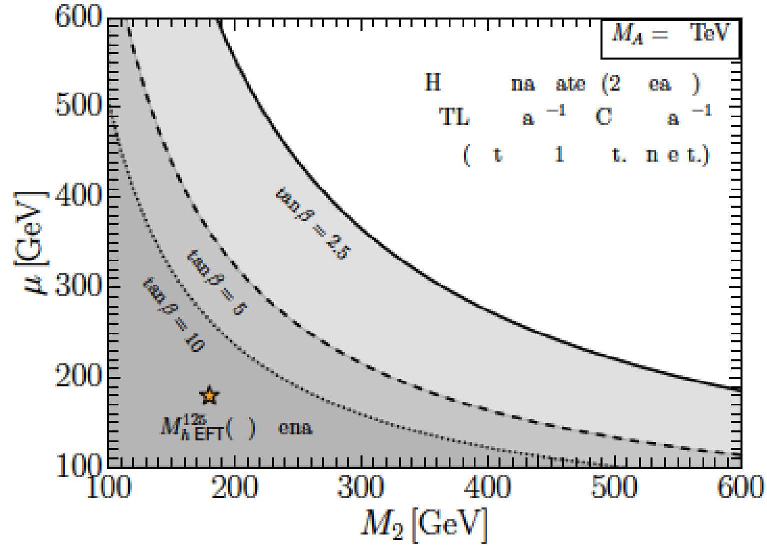

Figure 5: Projected reach of future Higgs signal rate measurements at ATLAS and CMS with 3 ab^{-1} assuming YR18 systematic uncertainties in the (M_2, μ) parameter plane around the $M_{h,\mathrm{EFT}}^{125}(\tilde{\chi})$ scenario (denoted by the orange star), for fixed $M_A = 3$ TeV. The solid, dashed and dotted contour lines and the corresponding gray areas indicate the 2σ reach for $\tan\beta$ values of 2.5, 5 and 10, respectively.

with the SM expectation. The results are shown for three different values of $\tan\beta = 2.5, 5, 10$ and fixed $M_A = 3\,\mathrm{TeV}$. As can be seen in Fig. 5, the reach in the chargino mass parameters M_2 and μ increases with decreasing $\tan\beta$, caused by a larger mixing of the charginos with decreasing $\tan\beta$, which directly impacts the $h \to \gamma\gamma$ partial decay width. Similarly, the largest values of the light chargino mass, $M_{\tilde{\chi}_1^\pm}$, can be probed if $M_2 \approx \mu$, as in this case the chargino mixing is large, and in turn, the Higgs boson coupling to charginos is maximized. For instance, for $\tan\beta = 2.5$ (5) and $M_2 \approx \mu$, light chargino masses up to ~ 255 (190) GeV can be probed at the 2σ level (in this case, the heavier chargino mass is ~ 410 (320) GeV). In contrast, in case of a larger hierarchy, $M_2 \gg \mu$ or $M_2 \ll \mu$, the smaller of the two mass parameters has to be rather low in order to be able to probe the electroweakino sector via the di-photon signal strength measurements. The nominal values of M_2 and μ that were chosen in the definition of the $M_{h,\mathrm{EFT}}^{125}(\tilde{\chi})$ scenario, marked by an orange star in Fig. 5, could be probed for $\tan\beta \lesssim 12.5$, which is in agreement with the findings in the $M_h^{125}(\tilde{\chi})$ scenario, see Fig. 3. We emphasize that this indirect probe for electroweakinos via their loop contributions to the $h \to \gamma\gamma$ partial decay width is complementary to the direct searches for electroweakinos at the HL-LHC [109].

Finally, in Fig. 6 we show the HL-LHC sensitivity for the proposed new $M_h^{125}(\mu = -2\,\mathrm{TeV})$ scenario in comparison with the M_h^{125} scenario and the other choices of $\mu = -1\,\mathrm{TeV}, -3\,\mathrm{TeV}$, as introduced in Section 2. The exclusion lines and filled regions are analogous to those in Fig. 1 (*left*), but are now determined using the HL-LHC prospective searches and measurements, instead of the current experimental results. The main qualitative features observed in Fig. 1

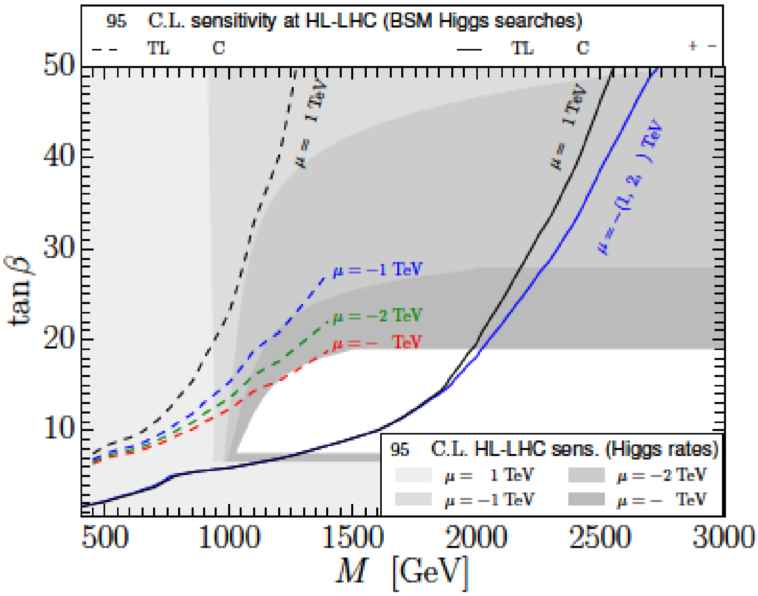

Figure 6: HL-LHC projections for the proposed new $M_h^{125}(\mu = -2\,\text{TeV})$ scenario in comparison with the M_h^{125} scenario and the other choices of $\mu = -1\,\text{TeV}, -3\,\text{TeV}$, shown in the $(M_A, \tan\beta)$ parameter plane; the dashed and solid lines show the expected exclusion from heavy Higgs boson searches in the $b\bar{b}$ and $\tau^+\tau^-$ final state, respectively, and the gray filled regions indicate the indirect reach of HL-LHC Higgs rate measurements.

(*left*) can be found here for the HL-LHC projections as well: Searches for heavy Higgs bosons in the $\tau^+\tau^-$ final state cover a larger area in the $(M_A, \tan\beta)$ parameter plane than those in the $b\bar{b}$ final state, and the $H/A \to b\bar{b}$ search sensitivity shows a strong dependence on the size and sign of μ while there is only a moderate impact on the searches in the $\tau^+\tau^-$ final state. On the other hand, Fig. 6 shows that the anticipated reach of heavy Higgs boson searches in the $b\bar{b}$ final state is competitive with the indirect reach of the anticipated Higgs-boson rate measurements. Except for $\mu = -3\,\text{TeV}$ the direct searches in the $b\bar{b}$ final state yield a stronger expected exclusion in the high-M_A region than the Higgs-boson rate measurements. The flat regions towards large values of M_A in the upper bounds on $\tan\beta$ for $\mu = -2\,\text{TeV}$ and $\mu = -3\,\text{TeV}$ are again caused by the fact that the prediction for the light Higgs-boson mass is below 122 GeV in this region (see Fig. 1 (*right*)), and the same applies to the lower limit in $\tan\beta$ (which is almost identical for all values of μ). However, for $M_A \lesssim 2\,\text{TeV}$ in the scenario with $\mu = -2\,\text{TeV}$ and for $M_A \lesssim 1.5\,\text{TeV}$ in the scenario with $\mu = -3\,\text{TeV}$ the Higgs rate measurements provide sensitivity for a non-trivial upper bound on $\tan\beta$.

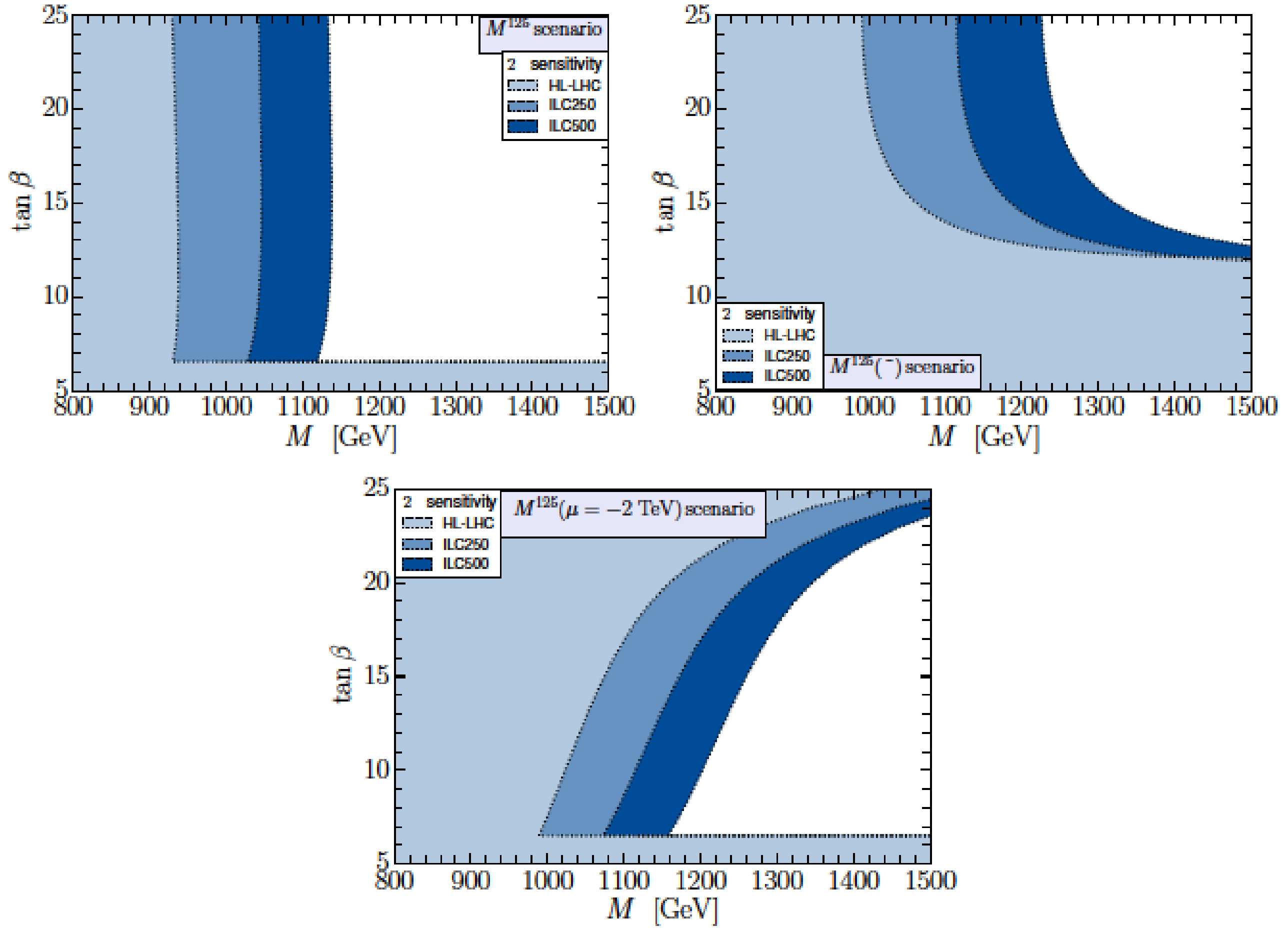

Figure 7: Prospective 2σ indirect exclusion region from Higgs rate measurements at the HL-LHC and the ILC, assuming agreement with the SM predictions, in the M_h^{125} scenario (upper left panel), the $M_h^{125}(\tilde{\chi})$ scenario (upper right panel), and the $M_h^{125,\mu-}$ scenario (bottom panel).

ments are included (see Sec. 3).

In the first two scenarios, M_h^{125} and $M_h^{125}(\tilde{\chi})$, the sensitivity at large $\tan\beta$ is determined by the decoupling behavior with M_A, resulting in roughly vertical exclusion lines for $\tan\beta \gtrsim 25$ (not explicitly shown in Fig. 7). In this large-$\tan\beta$ region the HL-LHC will already probe masses of the heavy Higgs bosons far in the decoupling regime, $M_A \gtrsim 920\,\text{GeV}$ and $1000\,\text{GeV}$ for the M_h^{125} and $M_h^{125}(\tilde{\chi})$ scenario, respectively. The ILC measurements at ILC250 and ILC500 will be able to extend the HL-LHC reach in M_A by around +(110–125) GeV and +(200–235) GeV, respectively. In the M_h^{125} scenario, due to the absence of light SUSY particles, this lower bound on M_A roughly remains the same for lower $\tan\beta$ values. These indirect constraints on M_A are complementary to the sensitivity of the direct searches discussed in Fig. 2, which depend on the details of the decay patterns of the heavy Higgs bosons. The indirect constraints from the rate measurements can potentially exceed the direct search sensitivity for heavy Higgs bosons

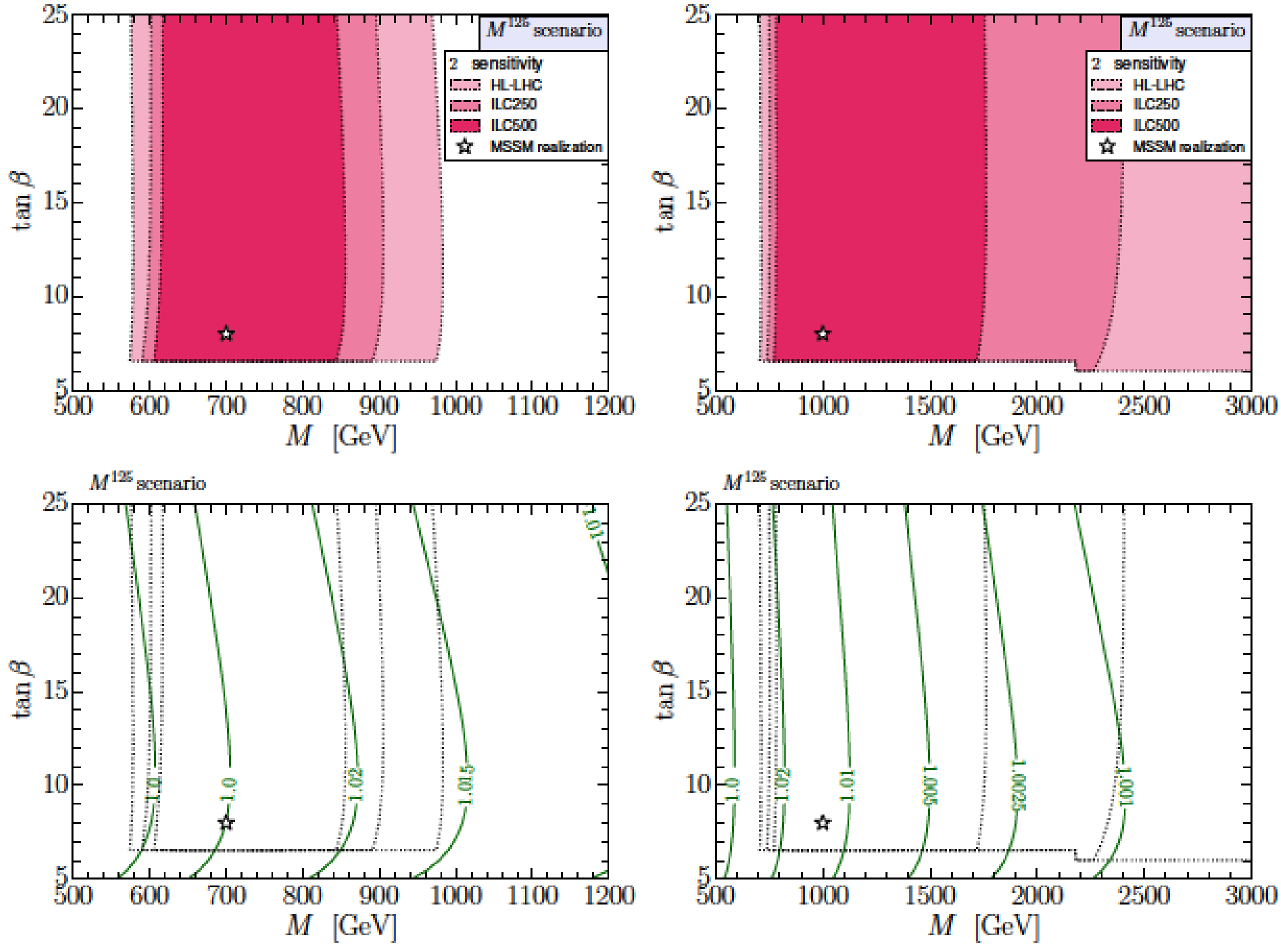

Figure 8: *Upper panels*: Indirect 2σ constraints in the $(M_A, \tan\beta)$ parameter plane of the M_h^{125} scenario from prospective Higgs-boson signal-rate measurements at the HL-LHC (faint red) and in combination with ILC250 (medium red) and ILC500 (bright red) measurements, assuming that the point, indicated by a star, $(M_A, \tan\beta) = (700\,\text{GeV}, 8)$ (left panel) or $(M_A, \tan\beta) = (1\,\text{TeV}, 8)$ (right panel) is realized in nature. *Lower panels*: SM-normalized Higgs rate in the $pp \to Vh, h \to b\bar{b}$ channel, R_{bb}^{Vh} (green contours), with the 2σ parameter ranges from the upper panels superimposed.

through the dependence of the involved branching ratio on the total width of the Higgs boson at 125 GeV. For instance, near the assumed points $(M_A, \tan\beta) = (700\,\text{GeV}, 8)$ and $(1000\,\text{GeV}, 8)$, the Higgs-to-diphoton rate is suppressed by 7% and 3% with respect to the SM prediction, respectively, as a result of a slightly enhanced bottom-quark Yukawa coupling and its impact on the total Higgs width. The combination of the measurements of the Higgs signal rates at the HL-LHC in various channels involving the product of the production cross sections and decay branching ratios will therefore provide sensitive information on possible deviations from the SM, while it will be non-trivial to disentangle the source of the deviations. Concerning

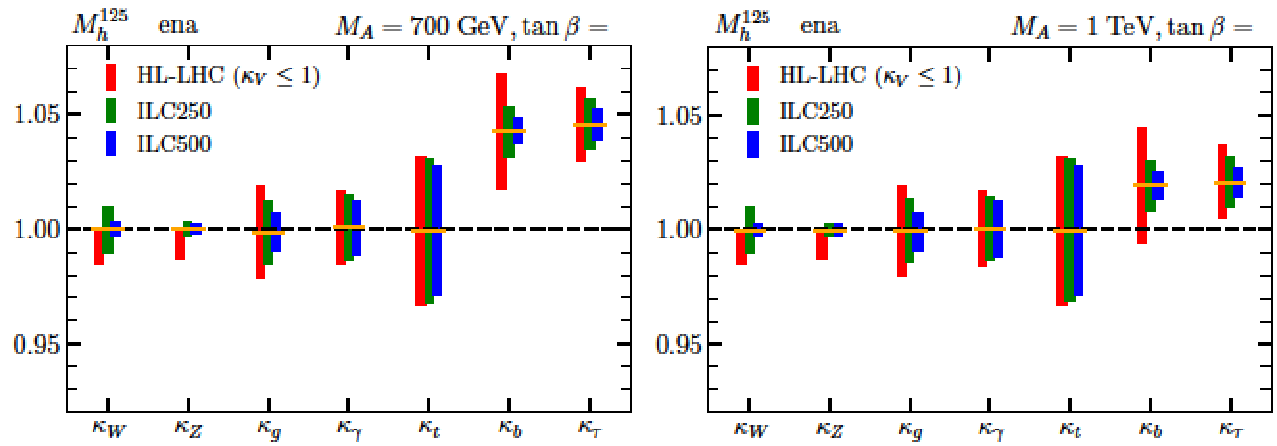

Figure 9: *Wäscheleinen-plots* for the two assumed MSSM parameter points $(M_A, \tan\beta) = (700\,\text{GeV}, 8)$ (left) and $(M_A, \tan\beta) = (1\,\text{TeV}, 8)$ (right) in the M_h^{125} scenario: Predicted Higgs couplings in the κ framework (orange horizontal bars) along with the anticipated 1σ precision from a global fit [104] to Higgs rate measurements at the HL-LHC, where the theoretical assumption $\kappa_V \leq 1$ is employed, and including prospective measurements at ILC250 and ILC500 (but without imposing an assumption on κ_V).

the prospective rate measurements at the ILC, the most precise Higgs rate measurements will be performed in the $e^+e^- \to Zh$, $h \to b\bar{b}$ channel during the run at 250 GeV and in the $e^+e^- \to \nu\bar{\nu}h$, $h \to b\bar{b}$ channel in the 500 GeV run [104], each with a precision at the sub-percent level. The ILC measurements will therefore complement the information obtainable at the HL-LHC with high-precision input on observables that cannot be well exploited at the LHC. The ILC will furthermore provide model-independent measurements of individual branching ratios. This kind of information will be crucial in order to determine the source of possible deviations without invoking model assumptions. In order to investigate the underlying nature of detected deviations from the SM, the indirect constraints that we have discussed here should of course be applied in the context of the information that is available from the direct searches for additional Higgs bosons (see in particular Fig. 2) and other states of new physics. The limits from these searches may in fact exclude large regions of the parameter space that is favored by the indirect constraints. Naturally, in case of a significant excess (or more than one) in the direct searches the prospects for narrowing down the possible nature of new physics with the combination of direct and indirect information would of course much improved.

The pattern of the deviations from the SM predictions corresponding to the situation where the parameter point $(M_A, \tan\beta) = (700\,\text{GeV}, 8)$ or the point $(M_A, \tan\beta) = (1000\,\text{GeV}, 8)$ of the M_h^{125} scenario is realized in nature is shown in Fig. 9. The displayed plots, which we denote as "*Wäscheleinen-plots*" (washing line plots) in the following, show the predicted light Higgs couplings (normalized to the SM prediction) at the assumed MSSM points in the κ framework [61], along with the anticipated 1σ precision of a rather general κ determination [104]

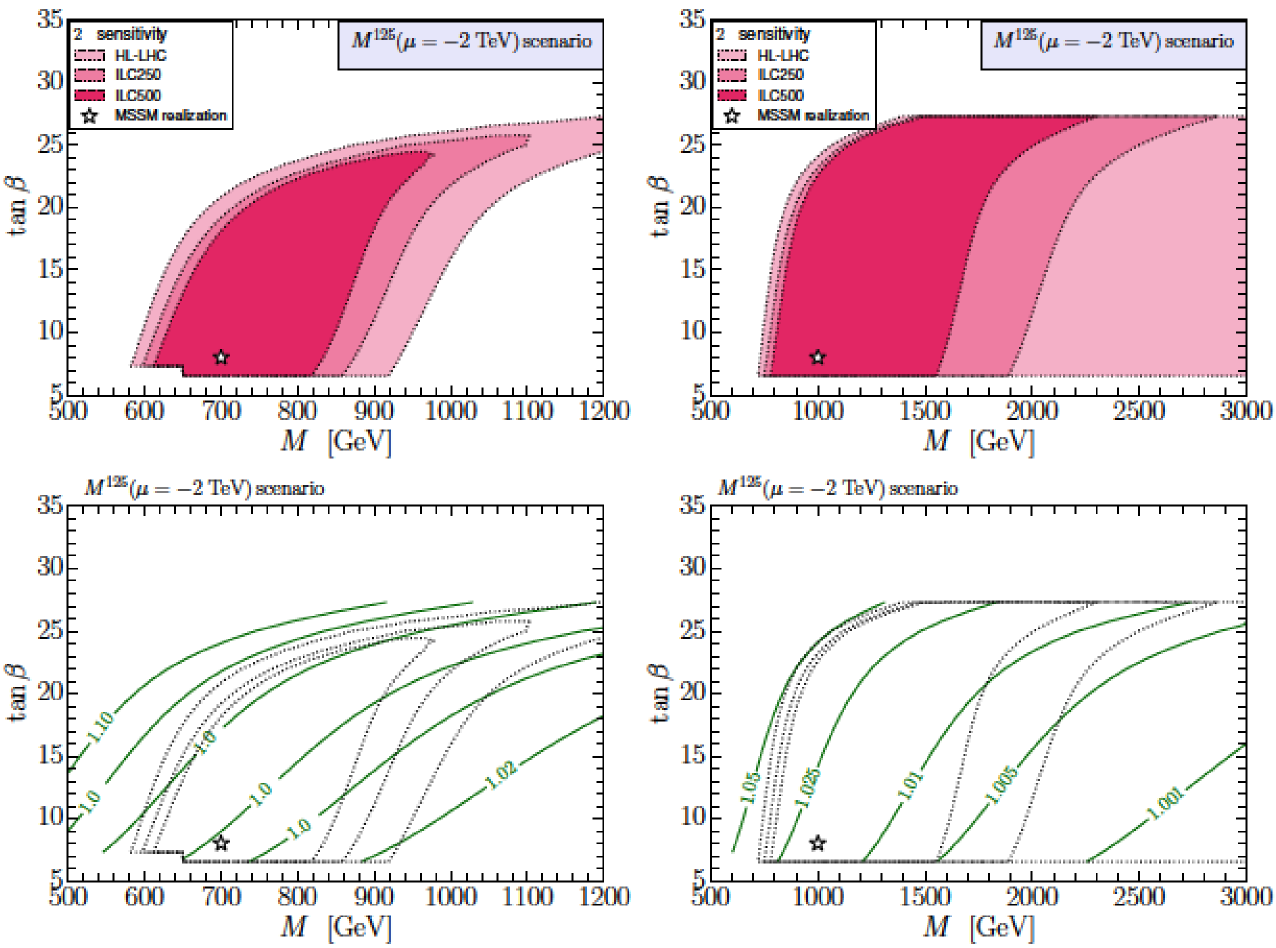

Figure 10: Indirect 2σ constraints in the $(M_A, \tan\beta)$ parameter plane from prospective Higgs-boson signal-rate measurements at the HL-LHC and the ILC (upper row) and R_{bb}^{Vh} contours (lower row) in the $M_h^{125,\mu-}$ scenario, assuming that the point, indicated by a star, $(M_A, \tan\beta) =$ (700 GeV, 8) (left panels) or $(M_A, \tan\beta) = (1\text{ TeV}, 8)$ (right panels) is realized in nature. The same color coding as in Fig. 8 is used.

from the SM. This kind of information will be crucial to determine the underlying nature of the detected deviations. As discussed above, those investigations should of course be based on both the direct information from searches and the indirect constraints. For the $M_h^{125,\mu-}$ scenario large parts of the parameter region that would be preferred by the prospective Higgs rate measurements are within the 2σ reach of heavy Higgs searches in the $\tau^+\tau^-$ and possibly even $b\bar{b}$ final states at the HL-LHC, see Fig. 6. A robust excess in these searches would provide clues for the mass scale of the heavy Higgs bosons, M_A. The 125 GeV Higgs rate measurements could then, together with first potential measurements of the strength of such a heavy Higgs boson signal, allow one to put new physics interpretations under scrutiny and, within the considered scenario, lead to strongly improved constraints on the model parameters.

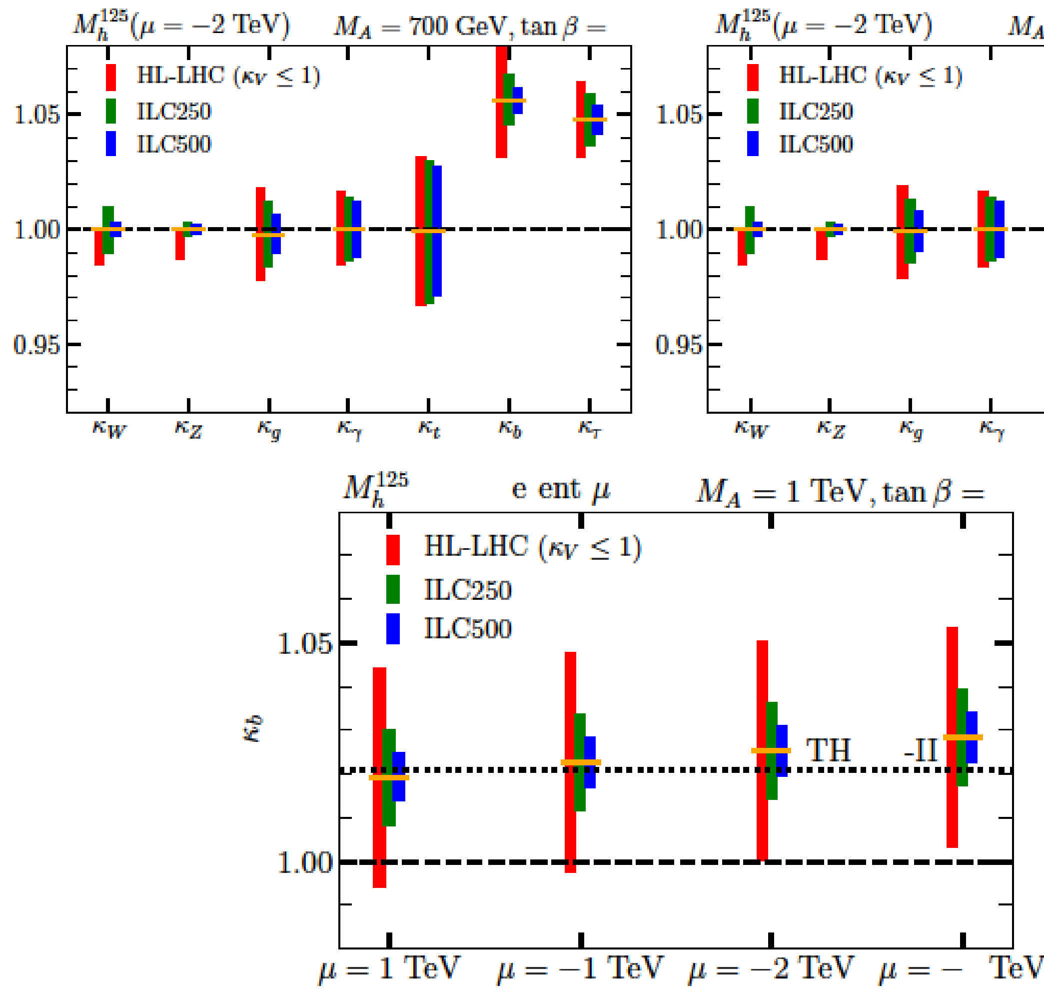

Figure 11: *Wäscheleinen-plots*, using the the same color coding as in Fig. 9, for the two assumed MSSM parameter points $(M_A, \tan\beta) = (700\,\text{GeV}, 8)$ (upper left panel) and $(M_A, \tan\beta) = (1\,\text{TeV}, 8)$ (upper right panel) in the $M_h^{125,\mu-}$ scenario. The lower panel shows for the assumed point $(M_A, \tan\beta) = (1\,\text{TeV}, 8)$ and different values of μ the prospects for κ_b, where for comparison also the corresponding prediction in the THDM-II (see text) is indicated (dotted line), see text for details. The Higgs couplings in the κ framework predicted in the displayed scenarios are compared with the anticipated 1σ precision from Higgs rate measurements, where at the HL-LHC the theoretical assumption $\kappa_V \leq 1$ is employed, while for the results including prospective measurements at ILC250 and ILC500 no assumption on κ_V is employed.

In Fig. 11 we show *Wäscheleinen-plots* for the parameter points $(M_A, \tan\beta) = (700\,\text{GeV}, 8)$ (upper left panel) and $(M_A, \tan\beta) = (1000\,\text{GeV}, 8)$ (upper right panel) in the $M_h^{125,\mu-}$ scenario, i.e. we show the predicted Higgs couplings represented by κ scale factors in the displayed scenarios along with the prospective 1σ precision levels of their determination from a global fit [104] to Higgs rate measurements. For the precisions from HL-LHC the theoretical assumption $\kappa_V \leq 1$

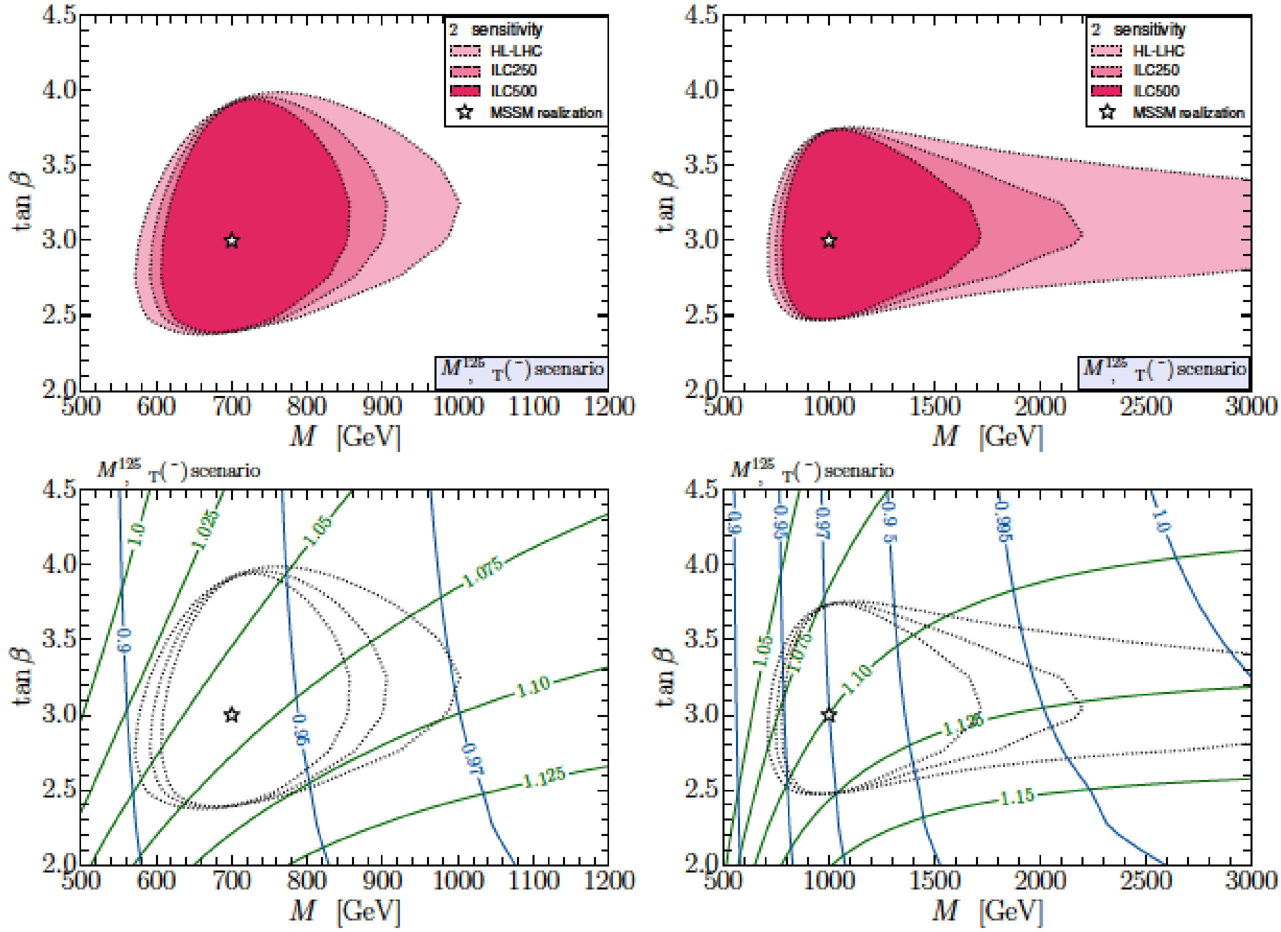

Figure 12: Indirect 2σ constraints in the $(M_A, \tan\beta)$ parameter plane of the $M_{h,\text{EFT}}^{125}(\tilde{\chi})$ scenario from prospective Higgs-boson signal-rate measurements at the HL-LHC and the ILC (upper row) and contours for SM-normalized Higgs rates (lower row) with the same color coding as in Fig. 8, assuming that the point, indicated by a star, $(M_A, \tan\beta) = (700\,\text{GeV}, 3)$ (left panel) or $(M_A, \tan\beta) = (1\,\text{TeV}, 3)$ (right panel) is realized in nature. The blue and green contours in the lower panels show the inclusive rate for $pp \to h \to VV$ $(V = W^\pm, Z)$, R^h_{VV}, and the inclusive rate for $pp \to h \to \gamma\gamma$, $R^h_{\gamma\gamma}$, respectively, with the 2σ parameter ranges from the upper panels superimposed.

of $\tan\beta$ in the electroweakino sector and can thus provide complementary information [109].

In Fig. 12 we show the results in the $M_{h,\text{EFT}}^{125}(\tilde{\chi})$ scenario, with the assumed parameter point $(M_A, \tan\beta) = (700\,\text{GeV}, 3)$ in the left panels, and $(M_A, \tan\beta) = (1000\,\text{GeV}, 3)$ in the right panels. The expected 2σ allowed parameter ranges obtained by Higgs-boson signal-rate measurements are shown in the upper panel of Fig. 12 with the same color coding as before in Figs. 8 and 10. The indirect bounds from the Higgs rate measurements on M_A for the first

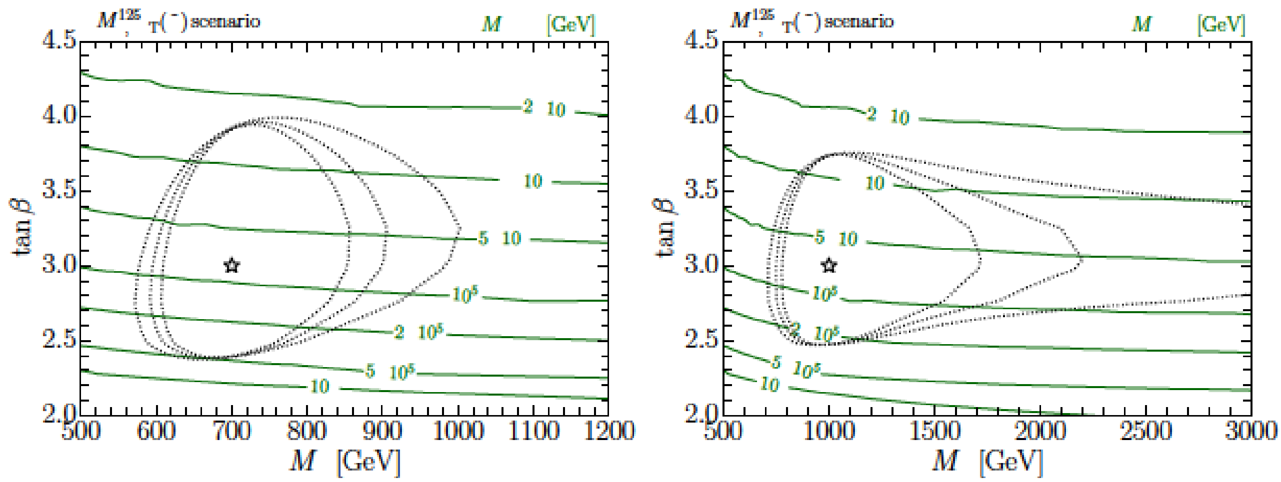

Figure 13: Contours of the scalar fermion soft-SUSY breaking mass $M_{\rm SUSY}$ in the (M_A, $\tan\beta$) parameter plane of the $M_{h,{\rm EFT}}^{125}(\tilde{\chi})$ scenario discussed in Fig. 12, assuming that the point, indicated by a star, $(M_A, \tan\beta) = (700\,{\rm GeV}, 3)$ (left panel) or $(M_A, \tan\beta) = (1\,{\rm TeV}, 3)$ (right panel) is realized in nature. The indirect 2σ constraints from prospective Higgs-boson signal-rate measurements at the HL-LHC and the ILC obtained in the upper panels of Fig. 12 are superimposed.

assumed point at $M_A = 700$ GeV ($\sim 6.5\%$, left plot). This is because at lower M_A values the enhancement of the $h \to b\bar{b}$ decay is stronger, which in turn suppresses the $h \to \gamma\gamma$ decay rate via its contribution to the total decay width. For the considered scenario the impact of the Higgs rate measurements at the ILC would mainly be a significant improvement of the indirect constraints on M_A.

In Fig. 13 we show contour lines of equal $M_{\rm SUSY}$ in the same parameter space as considered in Fig. 12. Superimposed (as dotted lines) are the expected 2σ-allowed parameter regions shown previously in Fig. 12 for the same MSSM points that we assume to be realized. $M_{\rm SUSY}$ denotes the scale of all scalar fermion soft-SUSY breaking masses. As explained in Sec. 2, in the $M_{h,{\rm EFT}}^{125}(\tilde{\chi})$ scenario $M_{\rm SUSY}$ is adjusted at every point in the parameter plane such that $M_h \simeq 125$ GeV. Thus the constraints in the $(M_A, \tan\beta)$ parameter plane for a given assumed realization of the MSSM can be translated into a constraint on the sfermion mass scale in this scenario. As a result, if such a scenario with light electroweakinos and a rather low value of $\tan\beta$ was realized in nature, the sensitivity to $\tan\beta$ arising from the loop contributions of the light charginos to the di-photon rate could be exploited to constrain $M_{\rm SUSY}$ to the ranges

$$2.3\,{\rm TeV} \lesssim M_{\rm SUSY} \lesssim 50\,{\rm TeV} \qquad \text{for } (M_A, \tan\beta) = (700\,{\rm GeV}, 3),$$

$$2.3\,{\rm TeV} \lesssim M_{\rm SUSY} \lesssim 30\,{\rm TeV} \qquad \text{for } (M_A, \tan\beta) = (1000\,{\rm GeV}, 3).$$

Those indirect constraints could of course be significantly improved with the results of the direct searches for additional Higgs bosons and electroweakinos, which in the considered scenario would have good prospects for a significant excess or even a discovery.

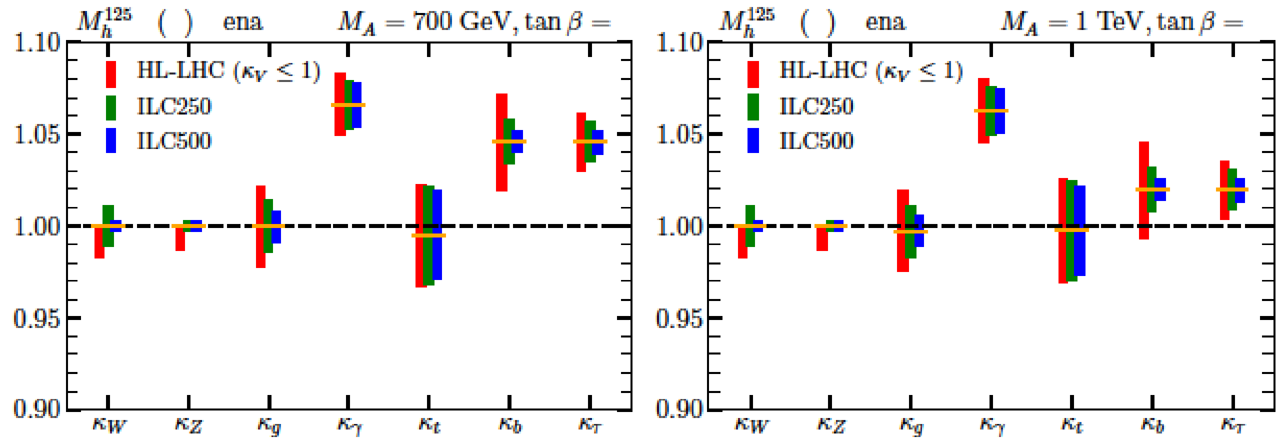

Figure 14: *Wäscheleinen-plots*, using the the same color coding as in Fig. 9, for the two assumed MSSM parameter points $(M_A, \tan\beta) = (700\,\text{GeV}, 3)$ (left panel) and $(M_A, \tan\beta) = (1\,\text{TeV}, 3)$ (right panel) in the $M_{h,\text{EFT}}^{125}(\tilde{\chi})$ scenario. The predicted Higgs couplings in the κ framework are compared with the anticipated 1σ precision from Higgs rate measurements, where at the HL-LHC the theoretical assumption $\kappa_V \leq 1$ is employed, while for the results including prospective measurements at ILC250 and ILC500 no assumption on κ_V is employed.

The predicted Higgs couplings in the $M_{h,\text{EFT}}^{125}(\tilde{\chi})$ scenario, parametrized in terms of κ scale factors, are shown in Fig. 14 for the assumed MSSM points $(M_A, \tan\beta) = (700\,\text{GeV}, 3)$ (left panel) and $(M_A, \tan\beta) = (1\,\text{TeV}, 3)$ (right panel) in comparison to the anticipated 1σ precision of the future κ determination. In contrast to the M_h^{125} scenario, Fig. 9, and in line with the previous discussion, because of the large loop contributions of the light charginos to the di-photon rate in the $M_{h,\text{EFT}}^{125}(\tilde{\chi})$ scenario a sizable deviation in κ_γ is clearly visible already with the HL-LHC precision. This precision on the effective Higgs-photon-photon coupling can only mildly be improved by the ILC measurements. On the other hand, κ_b and κ_τ show deviations similar to the points considered in the M_h^{125} scenario, Fig. 9, and here the ILC measurements will be crucial to achieve a significant discrimination with respect to the SM prediction.

We now turn to the discussion of the case that a relatively large value of $\tan\beta$ could be realized in nature. For this purpose we choose a heavy Higgs-boson mass of $M_A = 1.75\,\text{TeV}$. In the M_h^{125} and $M_h^{125}(\tilde{\chi})$ scenarios the $\tan\beta$ value is chosen to be $\tan\beta = 50$, close to the expected exclusion bound of the current $pp \to H/A \to \tau^+\tau^-$ analysis [65]. For the $M_h^{125,\mu-}$ scenario we fix $\tan\beta = 25$, close to the current indirect exclusion from Higgs rate measurements. The chosen value of $M_A = 1.75\,\text{TeV}$ is a "best-case" scenario if the MSSM with a large value of $\tan\beta$ is realized, in the sense that it would certainly lead to a discovery of heavy Higgs bosons at the HL-LHC (see our discussion above of the projections in the different benchmark scenarios) and possibly even already in the near future.

For definiteness, we quote here the 13 TeV signal rates of the processes $pp \to H/A \to \tau^+\tau^-$ and $pp \to H/A \to b\bar{b}$, whose production is completely dominated by bottom-quark associated

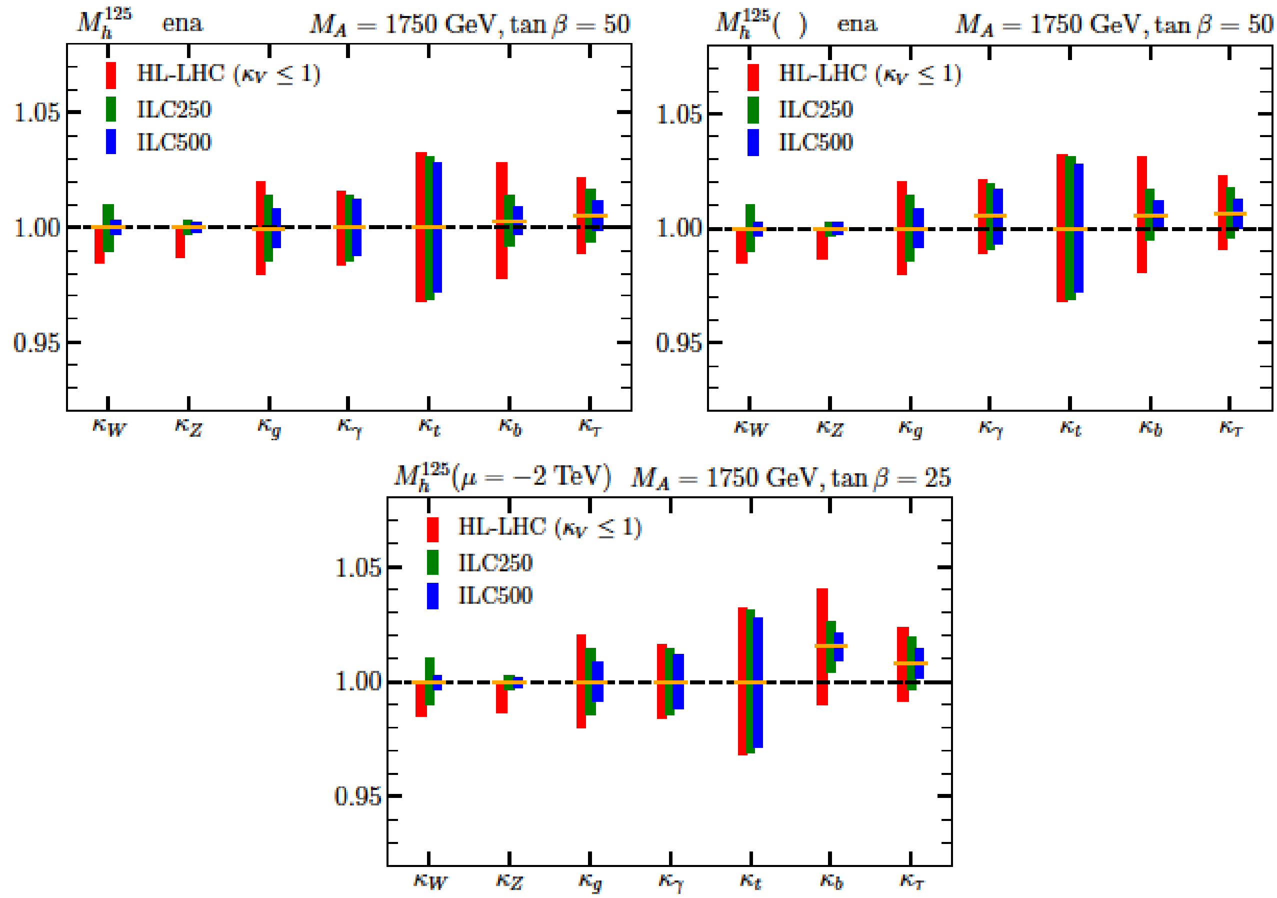

Figure 15: *Wäscheleinen-plots*, using the the same color coding as in Fig. 9, for the following three assumed MSSM scenarios: $(M_A, \tan\beta) = (1750\,\text{GeV}, 50)$ in the M_h^{125} scenario (upper left panel), $(M_A, \tan\beta) = (1750\,\text{GeV}, 50)$ in the $M_h^{125}(\tilde{\chi})$ scenario (upper right), and $(M_A, \tan\beta) = (1750\,\text{GeV}, 25)$ in the $M_h^{125,\mu-}$ scenario (lower panel). The predicted Higgs couplings in the κ framework are compared with the anticipated 1σ precision from Higgs rate measurements, where at the HL-LHC the theoretical assumption $\kappa_V \leq 1$ is employed, while for the results including prospective measurements at ILC250 and ILC500 no assumption on κ_V is employed.

used as null hypothesis). Here we want to focus on the latter. As the future measurements will naturally feature statistical fluctuations, we rather refer to the χ^2 of the SM hypothesis as $\Delta\chi^2_{\text{SM}} \equiv \chi^2_{\text{SM}} - \chi^2_{\text{MSSM}}$, where in our projection study with idealized measurements we have $\chi^2_{\text{MSSM}} = 0$ for the considered realized MSSM parameter point. In this likelihood ratio test between two simple hypotheses, with no adjustable model parameters, the levels $\Delta\chi^2 = 4$ and 9 correspond to a 2σ and 3σ tension, respectively, between the SM hypothesis and the MSSM hypothesis. It should be noted that this level of sensitivity does not allow one to exclude the SM hypothesis on grounds of the measurements alone, but instead only allows one to discriminate between two models. As these tensions are inferred *indirectly* from the signal rates of the

ATLAS *et al. Observation of a new particle in the search for the Standard Model Higgs boson with the ATLAS detector at the LHC* **B716** arXiv:1207.7214 [hep-ex]

CMS *et al. Observation of a New Boson at a Mass of 125 GeV with the CMS Experiment at the LHC* **B716** arXiv:1207.7235 [hep-ex]

ATLAS, CMS *et al. Measurements of the Higgs boson production and decay rates and constraints on its couplings from a combined ATLAS and CMS analysis of the LHC pp collision data at* ‾ *and 8 TeV* **08** arXiv:1606.02266 [hep-ex]

ATLAS *Combined measurements of Higgs boson production and decay using up to* *of proton–proton collision data at* ‾ *13 TeV collected with the ATLAS experiment* ATLAS-CONF-2019-005

CMS *et al. Measurement and interpretation of differential cross sections for Higgs boson production at* ‾ *13 TeV* **B792** arXiv:1812.06504 [hep-ex]

CMS *et al. Combined measurements of Higgs boson couplings in proton–proton collisions at* ‾ *TeV* **C79** arXiv:1809.10733 [hep-ex]

Supersymmetry, Supergravity and Particle Physics **110**

The Search for Supersymmetry: Probing Physics Beyond the Standard Model **117**

Higgs Bosons in Supersymmetric Models. 1. **B272**

et al. MSSM Higgs Boson Searches at the LHC: Benchmark Scenarios for Run 2 and Beyond **C79** arXiv:1808.07542 [hep-ph]

MSSM Higgs benchmark scenarios for Run 2 and beyond: the low region **C79** arXiv:1901.05933 [hep-ph]

et al. The CMSSM and NUHM1 after LHC Run 1 **C74** arXiv:1312.5250 [hep-ph]

Reduction of Couplings and its application in Particle Physics **814** arXiv:1904.00410 [hep-ph]

et al. Likelihood Analysis of the pMSSM11 in Light of LHC 13-TeV Data **C78** arXiv:1710.11091 [hep-ph]

et al. Report from Working Group 2 **7** arXiv:1902.00134 [hep-ph]

The CP conserving two Higgs doublet model: The Approach to the decoupling limit **D67** arXiv:hep-ph/0207010 [hep-ph]

Impersonating the Standard Model Higgs Boson: Alignment without Decoupling **04** arXiv:1310.2248 [hep-ph]

Complementarity between Nonstandard Higgs Boson Searches and Precision Higgs Boson Measurements in the MSSM **D91** arXiv:1410.4969 [hep-ph]

The Light and Heavy Higgs Interpretation of the MSSM **C77** arXiv:1608.00638 [hep-ph]

The Impact of Two-Loop Effects on the Scenario of MSSM Higgs Alignment without Decoupling **C77** arXiv:1708.04416 [hep-ph]

NMSSM interpretations of the observed Higgs signal **04** arXiv:1509.07283 [hep-ph]

Precise Predictions for the Higgs-Boson Masses in the NMSSM **C77** arXiv:1601.08100 [hep-ph]

Decays of the neutral Higgs bosons into SM fermions and gauge bosons in the -violating NMSSM **C78** arXiv:1807.06322 [hep-ph]

A 96 GeV Higgs boson in the N2HDM **C80** arXiv:1903.11661 [hep-ph]

Status of the Higgs Singlet Extension of the Standard Model after LHC Run 1 **75** arXiv:1501.02234 [hep-ph]

LHC Benchmark Scenarios for the Real Higgs Singlet Extension of the Standard Model **76** arXiv:1601.07880 [hep-ph]

Two-real-scalar-singlet extension of the SM: LHC phenomenology and benchmark scenarios **80** arXiv:1908.08554 [hep-ph]

FeynHiggs: A Program for the calculation of the masses of the neutral CP even Higgs bosons in the MSSM **124** arXiv:hep-ph/9812320 [hep-ph]

The Masses of the neutral CP - even Higgs bosons in the MSSM: Accurate analysis at the two loop level **C9** arXiv:hep-ph/9812472 [hep-ph]

Towards high precision predictions for the MSSM Higgs sector **C28** arXiv:hep-ph/0212020 [hep-ph]

The Higgs Boson Masses and Mixings of the Complex MSSM in the Feynman-Diagrammatic Approach **02** arXiv:hep-ph/0611326 [hep-ph]

High-Precision Predictions for the Light CP -Even Higgs Boson Mass of the Minimal Supersymmetric Standard Model **112** arXiv:1312.4937 [hep-ph]

Precise prediction for the light MSSM Higgs boson mass combining effective field theory and fixed-order calculations **C76** arXiv:1608.01880 [hep-ph]

Reconciling EFT and hybrid calculations of the light MSSM Higgs-boson mass **C78** arXiv:1706.00346 [hep-ph]

Precise prediction of the MSSM Higgs boson masses for low M_A **07** arXiv:1805.00867 [hep-ph]

Precision calculations in the MSSM Higgs-boson sector with FeynHiggs 2.14 arXiv:1811.09073 [hep-ph]

Theoretical uncertainties in the MSSM Higgs boson mass calculation arXiv:1912.04199 [hep-ph]

SusHi: A program for the calculation of Higgs production in gluon fusion and bottom-quark annihilation in the Standard Model and the MSSM **184** arXiv:1212.3249 [hep-ph]

SusHi Bento: Beyond NNLO and the heavy-top limit **212** arXiv:1605.03190 [hep-ph]

Higgs production and decay: Analytic results at next-to-leading order QCD **12** arXiv:hep-ph/0509189 [hep-ph]

Next-to-next-to-leading order Higgs production at hadron colliders **88** arXiv:hep-ph/0201206 [hep-ph]

Production of a pseudoscalar Higgs boson at hadron colliders at next-to-next-to leading order **10** arXiv:hep-ph/0208096 [hep-ph]

Higgs Boson GluonFfusion Production Beyond Threshold in N QCD **03** arXiv:1411.3584 [hep-ph]

Soft expansion of double-real-virtual corrections to Higgs production at N LO **08** arXiv:1505.04110 [hep-ph]

High precision determination of the gluon fusion Higgs boson cross-section at the LHC **05** arXiv:1602.00695 [hep-ph]

NLO QCD bottom corrections to Higgs boson production in the MSSM **11** arXiv:1007.3465 [hep-ph]

NLO QCD corrections to pseudoscalar Higgs production in the MSSM **08** arXiv:1107.0914 [hep-ph]

On the NLO QCD Corrections to the Production of the Heaviest Neutral Higgs Scalar in the MSSM **C72** arXiv:1204.1016 [hep-ph]

NLO Electroweak Corrections to Higgs Boson Production at Hadron Colliders **B670** arXiv:0809.1301 [hep-ph]

Resummation and matching of b-quark mass effects in $^{-}$ production **11** arXiv:1508.03288 [hep-ph]

Matched predictions for the $^{-}$ cross section at the 13 TeV LHC **10** arXiv:1605.01733 [hep-ph]

Higgs production in bottom-quark fusion in a matched scheme **B751** arXiv:1508.01529 [hep-ph]

Higgs production in bottom-quark fusion: matching beyond leading order **B763** arXiv:1607.00389 [hep-ph]

Supersymmetry and the Quark Mass Matrix **B303**

The Top quark mass in supersymmetric SO(10) unification **D50** arXiv:hep-ph/9306309 [hep-ph]

Yukawa coupling unification with supersymmetric threshold corrections **D49**

Electroweak symmetry breaking and bottom - top Yukawa unification **B426** arXiv:hep-ph/9402253 [hep-ph]

Effective Lagrangian for the interaction in the MSSM and charged Higgs phenomenology **B577** arXiv:hep-ph/9912516 [hep-ph]

and supersymmetry with large **B499** arXiv:hep-ph/0010003 [hep-ph]

MSSM Higgs Boson Searches at the LHC: Benchmark Scenarios after the Discovery of a Higgs-like Particle **C73** arXiv:1302.7033 [hep-ph]

LHC Higgs Cross Section Working Group *et al. Handbook of LHC Higgs Cross Sections: 4. Deciphering the Nature of the Higgs Sector* arXiv:1610.07922 [hep-ph]

Higgs Boson Couplings to Bottom Quarks: Two-Loop Supersymmetry-QCD Corrections **101** arXiv:0808.0087 [hep-ph]

Supersymmetric Higgs Yukawa Couplings to Bottom Quarks at next-to-next-to-leading Order **06** arXiv:1001.1935 [hep-ph]

ATLAS *et al. Search for heavy neutral Higgs bosons produced in association with -quarks and decaying to -quarks at TeV with the ATLAS detector* arXiv:1907.02749 [hep-ex]

CMS *et al. Search for additional neutral MSSM Higgs bosons in the final state in proton-proton collisions at 13 TeV* **09** arXiv:1803.06553 [hep-ex]

HiggsBounds: Confronting Arbitrary Higgs Sectors with Exclusion Bounds from LEP and the Tevatron **181** arXiv:0811.4169 [hep-ph]

HiggsBounds 2.0.0: Confronting Neutral and Charged Higgs Sector Predictions with Exclusion Bounds from LEP and the Tevatron **182** arXiv:1102.1898 [hep-ph]

Recent Developments in HiggsBounds and a Preview of HiggsSignals **CHARGED2012** arXiv:1301.2345 [hep-ph]

HiggsBounds *: Improved Tests of Extended Higgs Sectors against Exclusion Bounds from LEP, the Tevatron and the LHC* **C74** arXiv:1311.0055 [hep-ph]

Applying Exclusion Likelihoods from LHC Searches to Extended Higgs Sectors **C75** arXiv:1507.06706 [hep-ph]

HiggsBounds-5: Testing Higgs sectors in the LHC 13 TeV era

: Confronting arbitrary Higgs sectors with measurements at the Tevatron and the LHC **C74** arXiv:1305.1933 [hep-ph]

HiggsSignals-2: Probing new physics with precision Higgs measurements in the LHC 13 TeV era

ATLAS *et al. Combined measurements of Higgs boson production and decay using up to of proton-proton collision data at* ‾ *13 TeV collected with the ATLAS experiment* arXiv:1909.02845 [hep-ex]

CMS *et al. Measurements of properties of the Higgs boson decaying to a W boson pair in pp collisions at* ‾ *13 TeV* **B791** arXiv:1806.05246 [hep-ex]

CMS *Measurements of properties of the Higgs boson in the four-lepton final state in proton-proton collisions at* ‾ CMS-PAS-HIG-19-001

CMS *Measurements of Higgs boson production via gluon fusion and vector boson fusion in the diphoton decay channel at* ‾ *TeV*

CMS *et al. Search for the Higgs boson decaying to two muons in proton-proton collisions at* ‾ *13 TeV* **122** arXiv:1807.06325 [hep-ex]

CMS *Measurement of Higgs boson production and decay to the final state* CMS-PAS-HIG-18-032

CMS *et al. Evidence for the Higgs boson decay to a bottom quark–antiquark pair* **B780** arXiv:1709.07497 [hep-ex]

CMS *et al. Inclusive search for a highly boosted Higgs boson decaying to a bottom quark-antiquark pair* **120** arXiv:1709.05543 [hep-ex]

CMS *Measurement of* ‾ *production in the* ‾ *decay channel in of proton-proton collision data at* ‾ CMS-PAS-HIG-18-030

CMS *et al. Evidence for associated production of a Higgs boson with a top quark pair in final states with electrons, muons, and hadronically decaying leptons at* ‾ *13 TeV* **08** arXiv:1803.05485 [hep-ex]

CMS *Measurement of the associated production of a Higgs boson with a top quark pair in final states with electrons, muons and hadronically decaying leptons in data recorded in 2017 at* ‾ CMS-PAS-HIG-18-019

MSSM Higgs boson searches at the Tevatron and the LHC: Impact of different benchmark scenarios **C45** arXiv:hep-ph/0511023 [hep-ph]

CMS *Projection of the Run 2 MSSM H limits for the High-Luminosity LHC* CMS-PAS-FTR-18-017

Resonant heavy Higgs searches at the HL-LHC **09** arXiv:1812.05640 [hep-ph]

CMS *et al. Combination of searches for Higgs boson pair production in proton-proton collisions at* ‾ *13 TeV* **122** arXiv:1811.09689 [hep-ex]

Interference effects in the decays of spin-zero resonances into and ¯ **07** arXiv:1605.00542 [hep-ph]

Challenges and opportunities for heavy scalar searches in the ¯ *channel at the LHC* **11** arXiv:1608.07282 [hep-ph]

Signal background interference effects in heavy scalar production and decay to a top-anti-top pair **10** arXiv:1606.04149 [hep-ph]

Scalar production and decay to top quarks including interference effects at NLO in QCD in an EFT approach **10** arXiv:1707.06760 [hep-ph]

Production of heavy Higgs bosons and decay into top quarks at the LHC **D93** arXiv:1511.05584 [hep-ph]

Production of heavy Higgs bosons and decay into top quarks at the LHC. II: Top-quark polarization and spin correlation effects **D95** arXiv:1702.06063 [hep-ph]

Interference effects in ¯ *production at the LHC as a window on new physics* **03** arXiv:1901.03417 [hep-ph]

ATLAS *et al. Search for Heavy Higgs Bosons Decaying to a Top Quark Pair in Collisions at* ¯ *with the ATLAS Detector* **119** arXiv:1707.06025 [hep-ex]

CMS *Search for heavy Higgs bosons decaying to a top quark pair in proton-proton collisions at* ¯ CMS-PAS-HIG-17-027

The post-Higgs MSSM scenario: Habemus MSSM? **C73** arXiv:1307.5205 [hep-ph]

The MSSM Higgs sector at a high $_{SUSY}$*: reopening the low tan regime and heavy Higgs searches* **10** arXiv:1304.1787 [hep-ph]

Bounds to the Higgs Sector Masses in Minimal Supersymmetry from LHC Data **B724** arXiv:1305.2172 [hep-ph]

Fully covering the MSSM Higgs sector at the LHC **06** arXiv:1502.05653 [hep-ph]

The hMSSM approach for Higgs self-couplings revisited **C79** arXiv:1810.10979 [hep-ph]

Naturalness, the hyperbolic branch, and prospects for the observation of charged Higgs bosons at high luminosity LHC and 27 TeV LHC **D98** arXiv:1810.12868 [hep-ph]

et al. Higgs Boson Studies at Future Particle Colliders arXiv:1905.03764 [hep-ph]

et al. Theoretical uncertainties for electroweak and Higgs-boson precision measurements at FCC-ee arXiv:1906.05379 [hep-ph]

ATLAS *et al. Search for additional heavy neutral Higgs and gauge bosons in the ditau final state produced in of pp collisions at* ¯ *TeV with the ATLAS detector* **01** arXiv:1709.07242 [hep-ex]

ATLAS *et al. Search for heavy Higgs bosons decaying into two tau leptons with the ATLAS detector using collisions at* ¯ *TeV* arXiv:2002.12223 [hep-ex]

Heavy Higgs as a Portal to the Supersymmetric Electroweak Sector
04 arXiv:1811.11918 [hep-ph]

et al. Report from Working Group 3 **7**
arXiv:1812.07831 [hep-ph]

Precise prediction for the Higgs-boson masses in the
SSM **78** arXiv:1712.07475 [hep-ph]

International Workshop on Future Linear Collider (LCWS2017) Strasbourg, France, October 23-27, 2017 arXiv:1801.09662 [hep-ph]

International Large Detector Concept Group *Search for Light Scalars Produced in Association with a Z boson at the 250 GeV stage of the ILC* **ICHEP2018**

International Large Detector concept group
International Workshop on Future Linear Colliders (LCWS 2018) Arlington, Texas, USA, October 22-26, 2018
arXiv:1902.06118 [hep-ex]

Precise prediction for the Higgs-Boson masses in the
SSM with three right-handed neutrino superfields **79**
arXiv:1906.06173 [hep-ph]

Probing the Standard Model with
Higgs signal rates from the Tevatron, the LHC and a future ILC **11**
arXiv:1403.1582 [hep-ph]

LHC / LC interplay in the MSSM
Higgs sector **09** arXiv:hep-ph/0406322 [hep-ph]

LHC/LC Study Group *et al. Physics interplay of the LHC and the ILC*
426 arXiv:hep-ph/0410364 [hep-ph]

Improved
Formalism for Precision Higgs Coupling Fits **97** arXiv:1708.08912
[hep-ph]